Hindawi
Shock and Vibration
Volume 2020, Article ID 7831819, 12 pages
https://doi.org/10.1155/2020/7831819

Research Article

Analysis of Effective Operation Performance of Wireless Control Downhole Choke

Yukun Fu,[1] **Huiyun Ma**,[1] **Chenggang Yu**,[1] **Liangliang Dong**,[2] **Yunshan Yang**,[1] **Xiaohua Zhu**,[2] **and Hanwen Sun**[2]

[1]*Engineering Technology Research Institute, PetroChina Southwest Oil & Gas Field Company, Chengdu, Sichuan 610017, China*
[2]*School of Mechatronic Engineering, Southwest Petroleum University, Chengdu, Sichuan 610017, China*

Correspondence should be addressed to Yukun Fu; flyshand@126.com

Received 19 November 2019; Revised 24 August 2020; Accepted 20 October 2020; Published 12 November 2020

Academic Editor: Reza Kolahchi

Wireless control downhole throttle is designed to control the opening of downhole throttle remotely by ground pressure wave signal to regulate downhole production in a wireless and intelligent manner. The throttle's production regulation capability and the noise immunity of the signal receiver are the key factors affecting the reliability of the throttle operation. Based on computational fluid dynamics (CFD) theory, the flow field of downhole throttle is simulated numerically to study the flow resistance characteristics of wireless control downhole throttle and the stability of flow field at signal receiver. Finally, the field test proves that the tool achieves the design capacity of production regulation and can accurately receive signals to regulate downhole production in a wireless and intelligent manner. The research content of this paper provides theoretical and experimental basis for the further improvement and optimization of the wireless control downhole throttle's structure and has certain guiding significance for the field use of the throttle, achieving the purpose of downhole wireless intelligent production adjustment.

1. Introduction

Throttling production regulation is an important management step in the production process of gas wells and plays an important role in stabilizing production, conserving energy and reducing consumption, and assisting drainage and preventing hydrate formation [1–3]. In the natural gas production process, the downhole choke process installs the downhole choke at the preset position of the tubing to achieve wellbore throttling and pressure reduction. At the same time, it makes full use of the ground temperature to heat the choked natural gas flow so that the gas flow temperature after throttling is higher than the hydrate formation temperature under this pressure condition can achieve the purpose of reducing surface pipeline pressure, preventing hydrate formation, eliminating surface water jacket furnace, simplifying the surface process of the well site, quickly putting into production, and saving energy and reducing consumption.

At present, most of the downhole chokes used in gas wells are purely mechanical. When facing the smart completion mode, mechanical chokes have two major disadvantages. The first is that traditional downhole chokes are in the process of throttling; it is impossible to obtain real-time production data such as pressure and temperature before and after throttling. Second, the traditional downhole choke cannot adjust the size of the downhole nozzle diameter in real time. It is necessary to shut in the well and adopt rope operations to replace different sizes of nozzles to achieve different levels throttle function. According to incomplete statistics, during the period 2002 to 2019, the number of downhole choke salvage and replacement exceeded 250 well times. The operation time for a single choke replacement is about 4 to 5 days, which requires human and material resources such as operation team and well test truck, with long operation cycle and high cost. Therefore, there is an urgent need for a patented technology that can adjust the size of the downhole nozzle in real time without shutting in the well, so as to meet the needs of rapid adjustment of on-site

production, so as to ensure the safe and stable production of gas wells and improve the recovery rate. In recent years, with the maturity of mechatronics and digital intelligent technology, wireless control downhole throttling technology capable of production regulation by real-time remote control has become the development goal of oil and gas development and production management [4–11].

The wireless control throttle is the core of the wireless control downhole throttling technology, and determining its effective operation performance is of critical importance [12–23]. There are two key design points that affect the effective operation performance: noise immunity of the downhole signal receiver directly determines the reliability and accuracy of the remote wireless control of the entire system; the overall flow capacity of the throttle directly determines whether the gas can move smoothly. In order to optimize and improve the design of wireless control downhole choke valves and determine the effective performance of the tool, the author of this paper analyzes the flow capacity of the throttle and the noise immunity of the signal receiver. The main contents include the following. (1) The flow field analysis is carried out in the annular flow passage between the air guide cylinder and electric sealing cylinder. The flow area is changed by adjusting the diameter of the cylinder, and the critical flow cylinder diameter that meets the flow requirements is determined according to the characteristics of the annular flow resistance; when the cylinder diameter cannot meet the critical flow requirement due to restrictions of the size of the wellbore and other relevant parts, the critical effective working conditions of the throttle under different throttle opening and production before regulation are analyzed. (2) The monitor is mounted at the head end of the throttle to analyze the flow field characteristics at the signal receiver installed in the downhole flow field. Besides, we need to study and verify the reliability and accuracy of the downhole signal receiver for receiving ground pressure wave signal.

2. Structure and Principle of Wireless Control Downhole Throttle

The overall structure of the wireless control downhole throttle is shown in Figure 1. An orifice plate type valve capable of quantitatively adjusting the flow rate is used. And the opening of the throttle valve is controlled by the flap angle. The electric sealing cylinder is used to protect the internal electronic components and form an annular flow passage with the external air guiding cylinder. The head end is mounted with the downhole signal receiver for receiving the ground pressure wave signal. After decoding by the electronic component, it instructs the throttle valve flap to turn, adjusting the throttle opening and regulating production by remote wireless control.

3. Analysis of the Flow Capacity of the Annular Flow Passage between the Air Guide Cylinder and the Electric Sealing Cylinder

Due to the limited downhole space, the flow area of the annulus flow passage between the air guide cylinder and the electric sealing cylinder is small. When the production and the opening are large, the internal pressure drop of the tool may be greater than the pressure drop of the upper and lower ends of the tool, resulting in gas failure to pass and inconsistency between actual production and target production. Such condition has an impact on the reliability of the throttle operation. Simulation of the flow field distribution of the annulus flow passage between the air guide cylinder and the electric sealing cylinder is conducted herein. The characteristics of the annulus flow resistance under different working conditions are analyzed by adjusting the cylinder diameter, production before regulation, and the opening of the throttle valve. Thereafter, the critical flow cylinder diameter and critical effective working conditions are determined.

3.1. Simulation of Annulus Flow Field. The overall pressure drop of the throttle is 0.16 MPa by calculation on the conditions of production before regulation 200,000 m^3 and the angle of the flap 80°, that is, 100% opening. The flow field of the throttle is simulated under this pressure drop, and the flow velocity and dynamic pressure distribution between the throttle valve and the air guide cylinder and the electric sealing cylinder are analyzed, as shown in Figures 2 and 3.

3.2. Analysis of Critical Flow Cylinder Diameter of Annulus Flow Passage. Due to the strict requirements of the downhole space, the outer diameter of the throttle is restricted. The annular flow area must be changed when the inner diameter of the air guide cylinder remains unchanged, as shown in Figure 4.

Table 1 represents the flow pressure drop of the annular flow passage between the air guide cylinder and the electric sealing cylinder under different outer diameters of the electric sealing cylinder. It can be seen that when the outer diameter of the electric sealing cylinder is 36 mm, the flow pressure drop of the annular flow passage between the air guide cylinder and the electric sealing cylinder is lower than the flow pressure drop at 100% opening of the throttle valve. The middle and rear section of the throttle has a good flow capacity. Therefore, the outer diameter of the electric sealing cylinder should not be bigger than 36 mm.

3.3. Analysis of Critical Effective Operating Conditions of Throttle Valve. Due to the restriction of the size of the electronic components, the outer diameter of the electric sealing cylinder is not easily adjusted. In this section, we

Figure 1: Mechanical structure of wireless control throttle. 1, inlet nozzle; 2, static flap; 3, adapter sleeve; 4, valve body; 5, dynamic flap; 6, adapter sleeve; 7, electric sealing cylinder; 8, air guide cylinder; 9, fixing frame; 10, head; 11, sleeve.

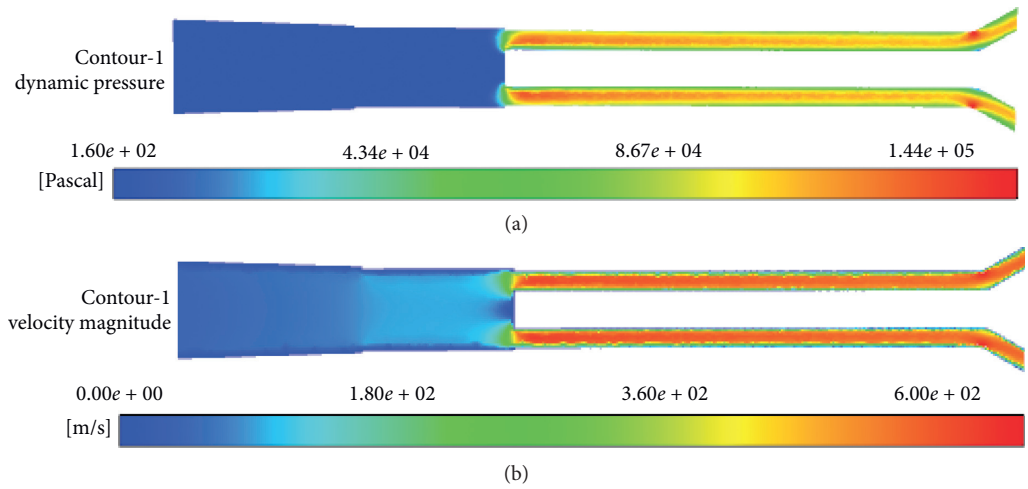

Figure 2: Distribution of front flow field of the throttle. (a) Dynamic pressure distribution. (b) Velocity distribution.

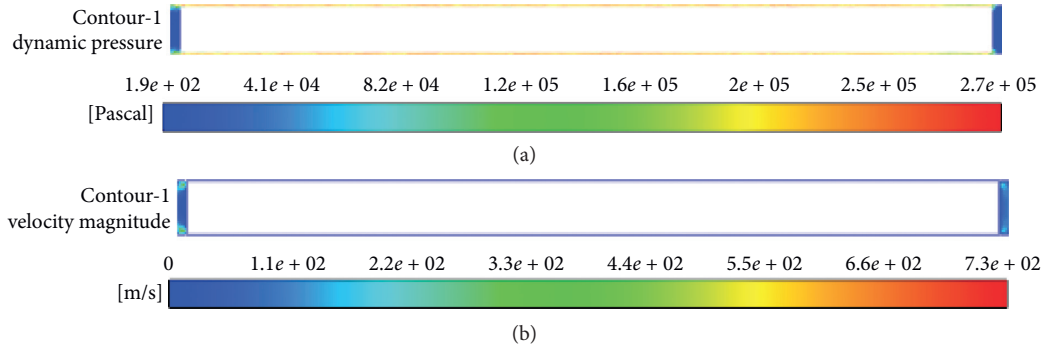

Figure 3: Distribution of flow field in annular flow passage. (a) Dynamic pressure distribution. (b) Velocity distribution.

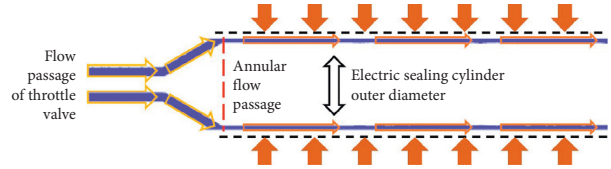

Figure 4: Change of the flow area of the annular flow passage.

analyze the effective working conditions when the throttle valve takes a leading role and if the outer diameter of the electric sealing cylinder is not up to the critical flow cylinder diameter.

Table 2 represents the annulus throttling pressure drop for different electric sealing cylinder outer diameters and production conditions before regulation. Table 3 represents the throttling pressure drop under different throttle valve flap angles and different production conditions before regulation. By comparing the annulus and the throttling pressure drop, the critical effective production and critical effective opening under the normal operation of the throttle valve are analyzed.

3.3.1. Critical Effective Production of Throttle Valve. When the flow area of the annulus flow passage is small, an excessively high production will make the throttling effect at

Table 1: Pressure drop corresponding to change of the outer diameter of the electric sealing cylinder.

Outer diameter of electric sealing cylinder (mm)	40.8	38	36	33	32	30
Pressure drop (MPa)	1.047	0.365	0.157	0.066	0.054	0.037

the annulus stronger than the throttle valve. In order to ensure that the throttling effect of the throttle valve takes lead in the overall throttling effect, the production before regulation should be lower than the critical effective production. Figure 5 represents the relation between the annular pressure drop and the throttling pressure drop of the fully open throttle valve with the change of production before regulation at different outer diameters of the electric seal cylinders. According to the figure, the throttling pressure drop of the annulus and the throttle valve decreases with the reduction of production before regulation. When the outer diameter of the electric sealing cylinder is 38 mm, the production before regulation is at least less than 10,000 m^3 so that the throttling pressure drop of the throttle valve can be higher than the annular throttling pressure drop; when the outer diameter of the electric sealing cylinder is 40.8 mm, the production before regulation is at least less than 4,000 m^3 so that the throttling effect of the throttle valve can take lead.

3.4. Critical Effective Opening of Throttle Valve. When the annular flow passage does not reach the optimal flow area, the critical effective production of the fully open throttle valve is low, which is difficult to achieve in actual production. Therefore, it is necessary to consider the opening range corresponding to the flap angle of the throttle valve with throttling pressure drop higher than the annular throttling pressure drop under the noncritical effective production, that is, the critical effective opening under a certain production.

Figure 6 represents the comparison of the annular pressure drop of the different outer diameters of electric sealing cylinder and the throttling pressure drop of the throttle valve of different openings under different productions before regulation. The opening range higher than the annular throttling pressure drop is the effective working opening range of the throttle valve under the current production before regulation. And the opening corresponding to the maximum flap angle is the critical effective opening under the current production.

Table 4 and Figure 7 represent the critical effective opening of the throttle valve under different productions before regulation and the outer diameters of electric sealing cylinder. According to the figure, the critical effective opening increases with the increasing production before regulation, and decreases with the increase of the outer diameter of the electric sealing cylinder, that is, reduction of the flow area of the annular flow passage. When the outer diameter of the electric sealing cylinder is 40.8 mm, the absolute critical effective opening is ~21°; when the value is 38 mm, the absolute critical effective opening is ~35.5°; when the value is 36 mm, the absolute critical effective opening can be up to 80° (100%). Thus, the critical effective opening increases as the outer diameter of the electric sealing cylinder decreases.

4. Simulation of Flow Field Stability at the Head End

The signal receiver mounted at the head end is an important part of wireless control, and its noise immunity is the guarantee of data reception accuracy [7]. In this section, the simulation of the flow field stability at the signal receiving area under different throttle valve openings and rated flow conditions is carried out to verify the noise immunity of the signal receiver. In addition, we draw the dynamic pressure fluctuation curve and the fluid trace diagram, analyze the dynamic pressure fluctuation trend, summarize the flow field dynamic pressure stabilization time, dynamic pressure fluctuation range, and mean value, and help commission the auxiliary signal receiver.

4.1. Monitor Establishment. In order to obtain information of the flow field of the head end in the numerical simulation of the throttle, a cylinder is arranged at the head end as a flow field monitor, as shown in Figure 8. The monitor is mounted adjacent to the signal receiver so that the flow field monitoring is more authentic.

4.2. Dynamic Pressure Fluctuations. Figures 9 and 10 represent the dynamic pressure curves of the flap angle of throttle valve at 10° and 80° under different rated productions. The figure includes the dynamic pressure fluctuation curve and the contour of the fluctuation range after stabilization, and the contour of the dynamic pressure mean value. According to the Figure, after the fluid flows in for a period of time, the flow field at the head end tends to be stable. When the opening of the throttle valve is small, the dynamic pressure stabilization time is basically ~4 s. When the throttle valve opening is relatively large, the time required for dynamic pressure stabilization is relatively small, with an average of ~3 s. And again, at the same throttle valve opening, the stabilization time decreases with the reduction of rated production. When the dynamic pressure is stabilized, the amplitude and range of dynamic pressure fluctuations increase nonlinearly with the ramping up of rated production. The larger the rated production, the larger the increase of dynamic pressure amplitude and fluctuation range. In contrast to the flap angle at 80° and 10°, the dynamic pressure fluctuation amplitude and range are also small under the same rated production. Under the rated flow of 50,000 m^3, the dynamic pressure is basically stable at the beginning.

Tables 5 and 6 represent the values of the dynamic pressure fluctuation range of the head end and the fluctuation mean value table under different rated productions and throttle valve openings. According to the table, after the flow field is stable, the dynamic pressure fluctuation amplitude and the mean value are not more than 50 Pa. The data

Table 2: Annular throttling pressure drop under different outer diameters of electric sealing cylinder.

Production	Electric sealing cylinder outer diameter (mm) Pressure drop (MPa)		
	40.8	39	38
50,000 m^3	0.079	0.045	0.024
100,000 m^3	0.291	0.221	0.162
150,000 m^3	0.623	0.392	0.231
200,000 m^3	1.047	0.701	0.365

Table 3: Throttling pressure drop at different throttling openings.

Production	Opening (°) Pressure drop (MPa)							
	10	20	30	40	50	60	70	80
50,000 m^3	0.43	0.1	0.04	0.025	0.017	0.013	0.011	0.01
100,000 m^3	1.7	0.4	0.168	0.09	0.071	0.05	0.044	0.042
150,000 m^3	3.82	0.91	0.38	0.212	0.14	0.108	0.095	0.092
200,000 m^3	6.77	1.61	0.68	0.372	0.246	0.188	0.169	0.16

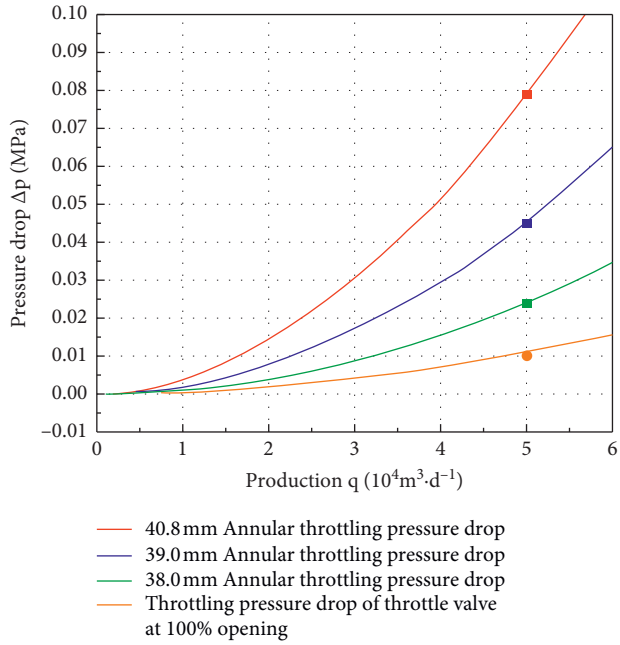

Figure 5: Comparison of annular pressure drop and pressure drop of fully open throttle valve.

acquisition range of the signal receiver can be adjusted by the maximum and minimum values of the dynamic pressure fluctuation so as to enhance data acquisition efficiency.

4.3. Motion Trace Diagram. Figures 11 and 12 represent dynamic pressure trace diagrams of the head end at different openings and productions. According to the trace diagram, the dynamic pressure is basically stable when the fluid flows through the head end. Under different rated flow rates and throttle valve openings, the dynamic pressure at the head end of the downhole sensor fluctuates after the flow stabilizes. When the throttle valve is used, the fluid becomes stable once getting out of the throttle nozzle, and basically no turbulent flow is formed. Such scenario has little influence on the receiving data of the downhole signal receiver, and the reliability of data reception can be guaranteed.

5. Field Test of Wireless Control Throttle

In order to verify that the wireless control throttle designed herein can run smoothly, 7 wells times are scheduled for production regulation in the southwest oil and gas field. Figure 13 represents the opening of the throttle valve before and after the pressure wave signal is sent on the well. In the

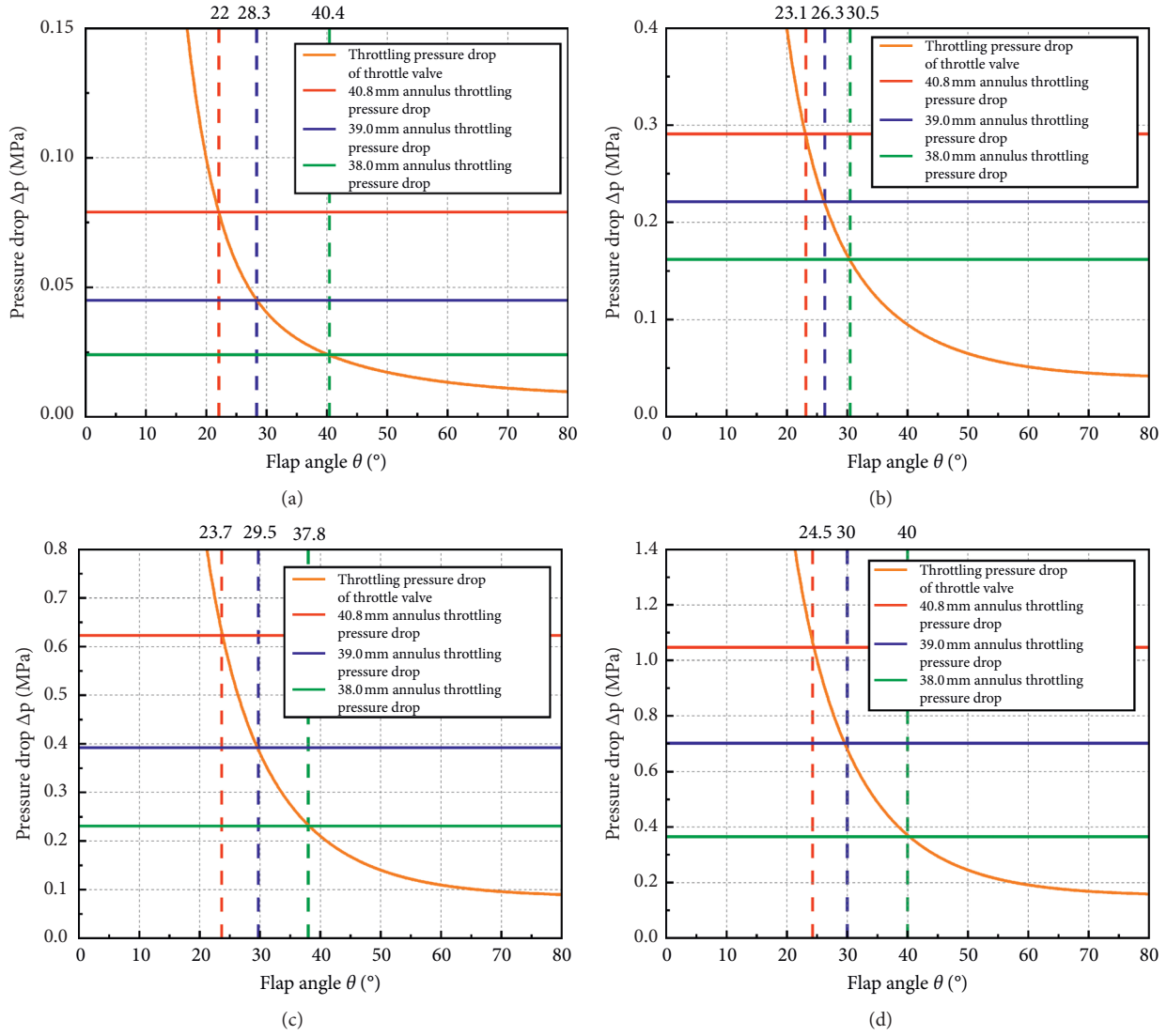

Figure 6: Comparison of annular pressure drop and pressure drop of throttle valve with different openings. (a) 50,000 m^3. (b) 100,000 m^3. (c) 150,000 m^3. (d) 200,000 m^3.

Table 4: Critical effective opening of throttle valve.

Production	Outer diameter of electric sealing cylinder (mm) Opening (°)		
	40.8	39	38
50,000 m^3	22	28.3	40.4
100,000 m^3	23.1	26.3	30.5
150,000 m^3	23.7	29.5	37.8
200,000 m^3	24.5	30	40

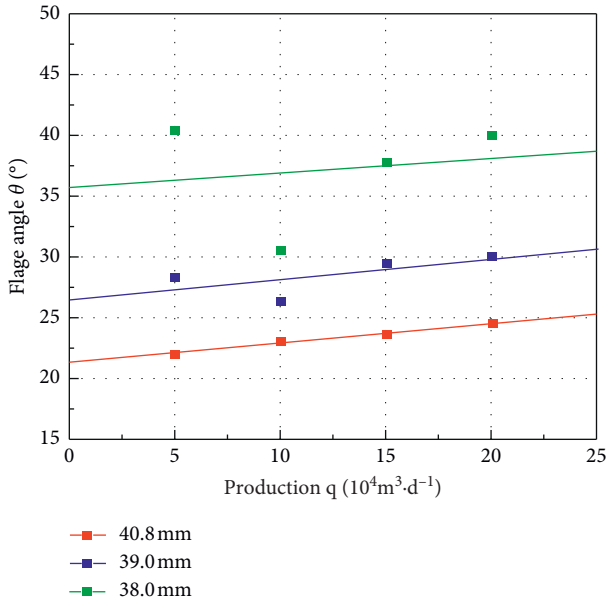

Figure 7: Relation between critical effective opening and production before regulation.

Figure 8: Position of monitor in the head end.

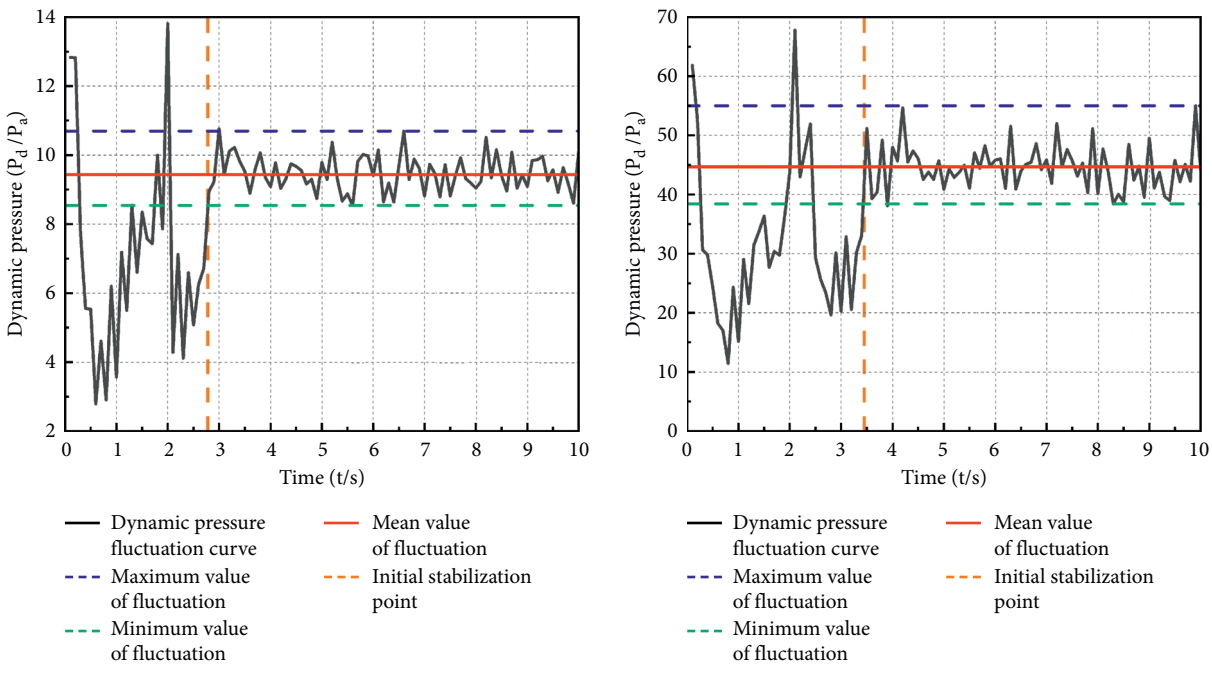

Figure 9: Continued.

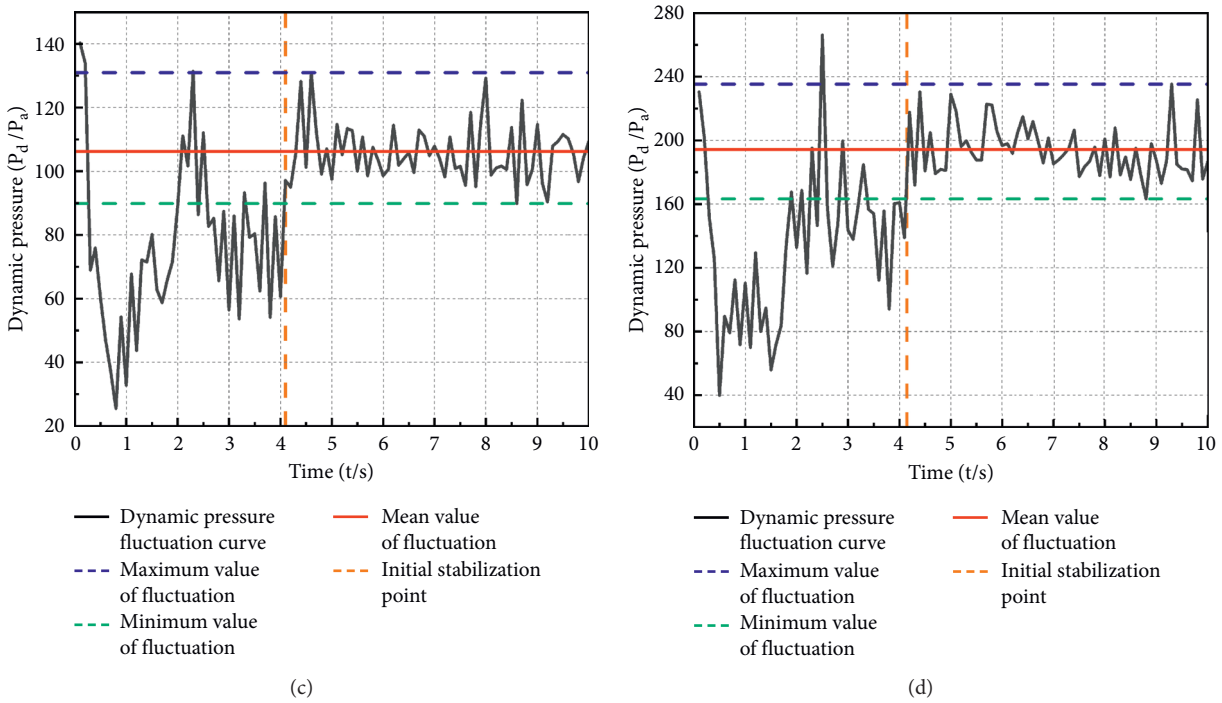

Figure 9: Dynamic pressure curve of sensor head end with flap angle at 10°. (a) 50,000 m^3. (b) 100,000 m^3. (c) 150,000 m^3. (d) 200,000 m^3.

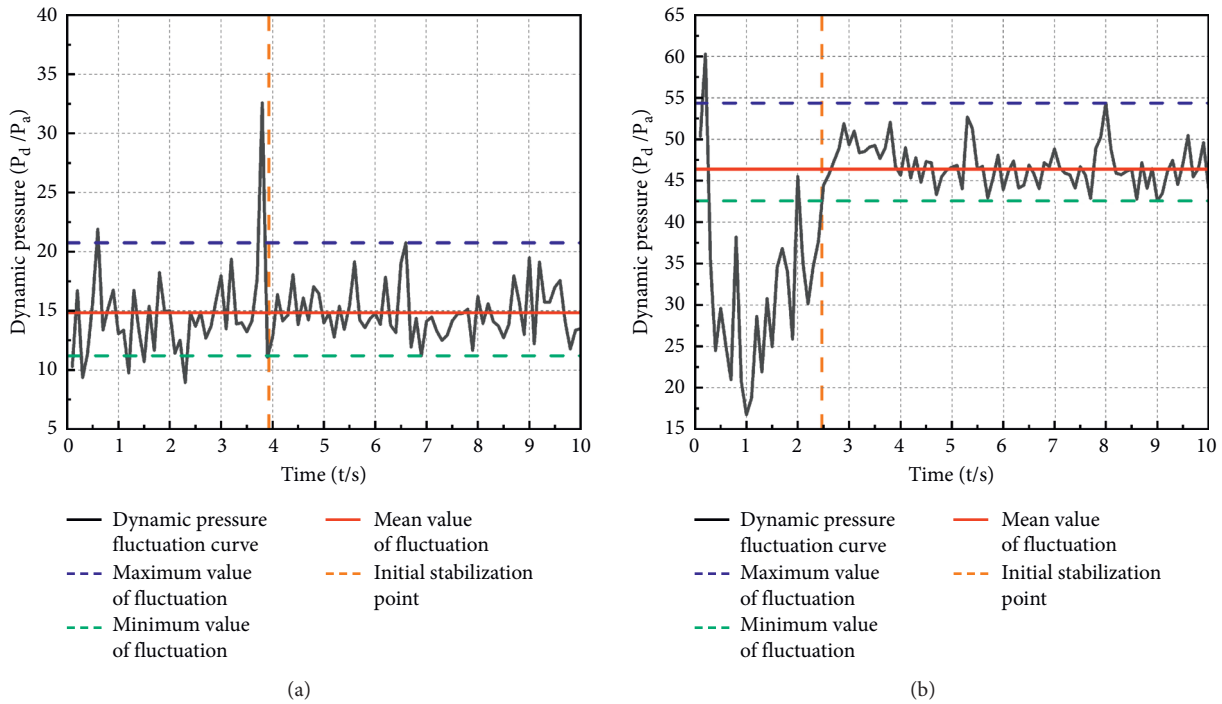

Figure 10: Continued.

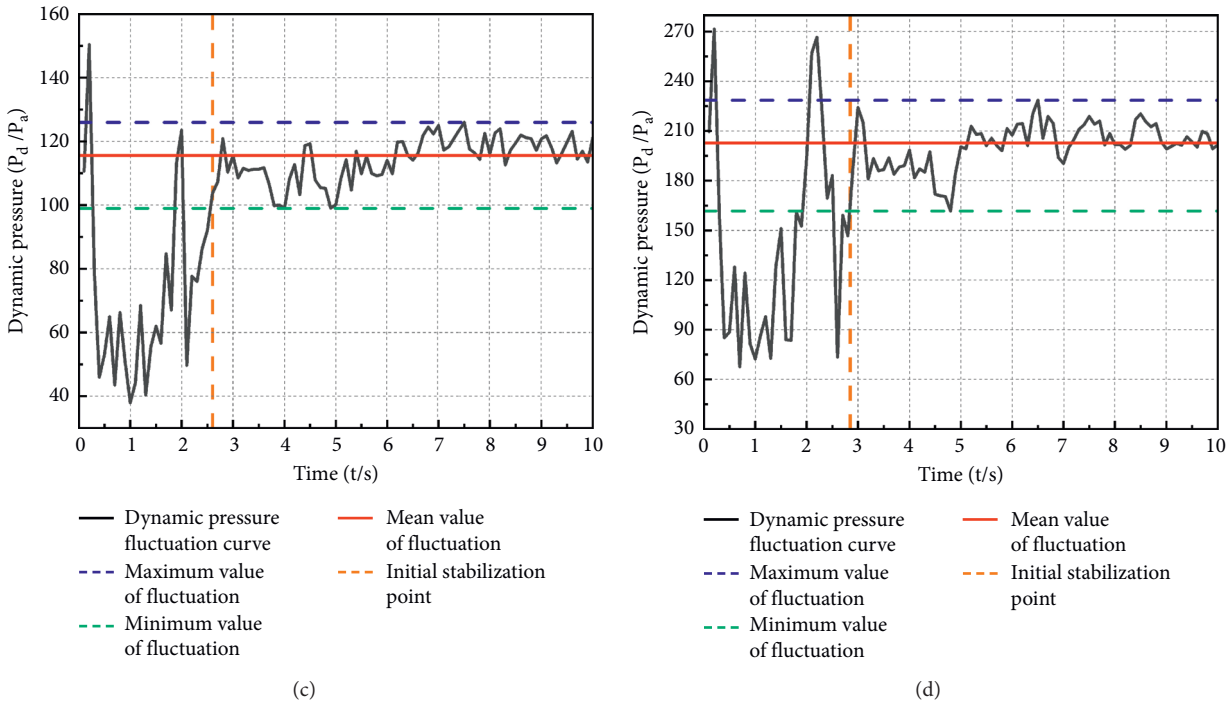

Figure 10: Dynamic pressure curve of sensor head end with flap angle at 80°. (a) 50,000 m^3. (b) 100,000 m^3. (c) 150,000 m^3. (d) 200,000 m^3.

Table 5: Dynamic pressure fluctuation scope at 10° flap angle.

	50,000 m^3	100,000 m^3	150,000 m^3	200,000 m^3
Fluctuation scope (Pa)	8.538–10.6971	38.4311–55.0196	89.8664–130.9628	163.2572–235.3277
Fluctuation average value (Pa)	9.4362	44.6898	106.2321	194.2762

Table 6: Dynamic pressure fluctuation scope at 80° flap angle.

	50,000 m^3	100,000 m^3	150,000 m^3	200,000 m^3
Fluctuation scope (Pa)	11.2045–20.7428	42.5521–54.3737	99.0038–125.9852	161.7224–228.4959
Fluctuation average value (Pa)	14.8451	46.3893	115.5894	202.8745

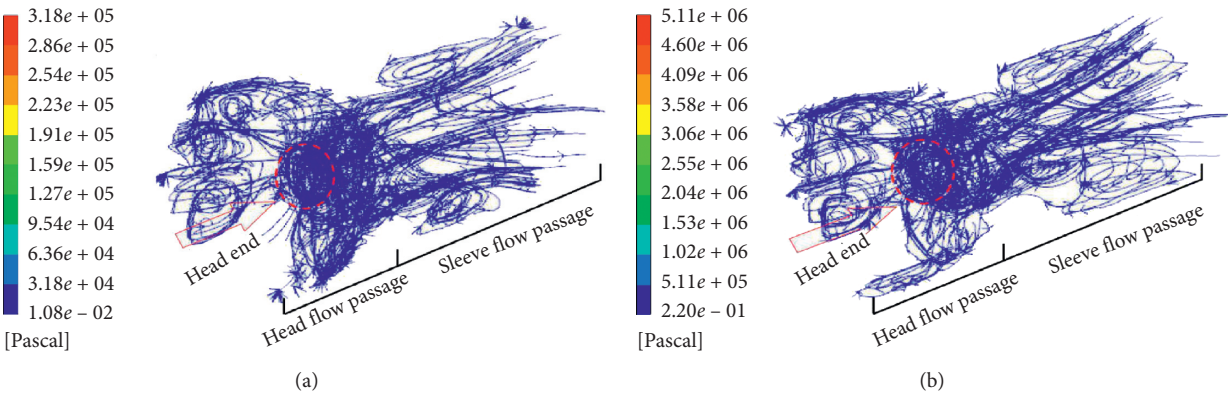

Figure 11: Head end trace diagram at 10° flap angle. (a) 50,000 m^3. (b) 200,000 m^3.

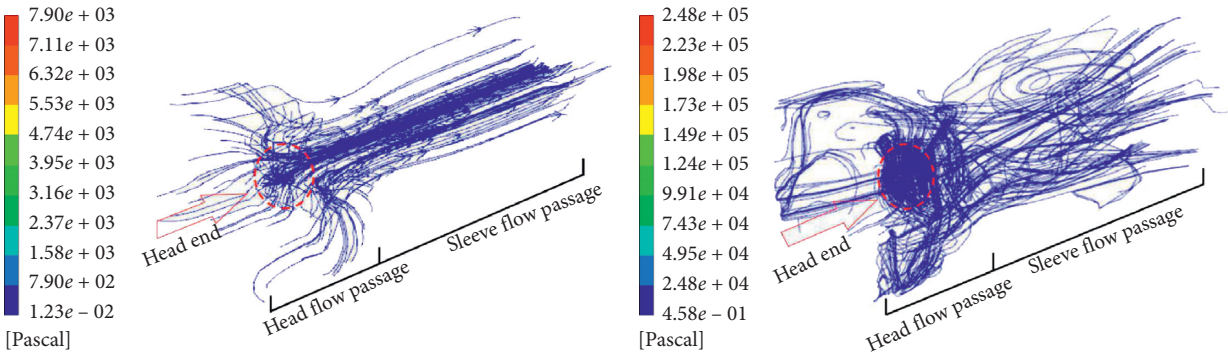

(a) (b)

Figure 12: Head end trace diagram at 80° flap angle. (a) 50,000 m^3. (b) 200,000 m^3.

(a) (b)

Figure 13: Valve opening before field production regulation test.

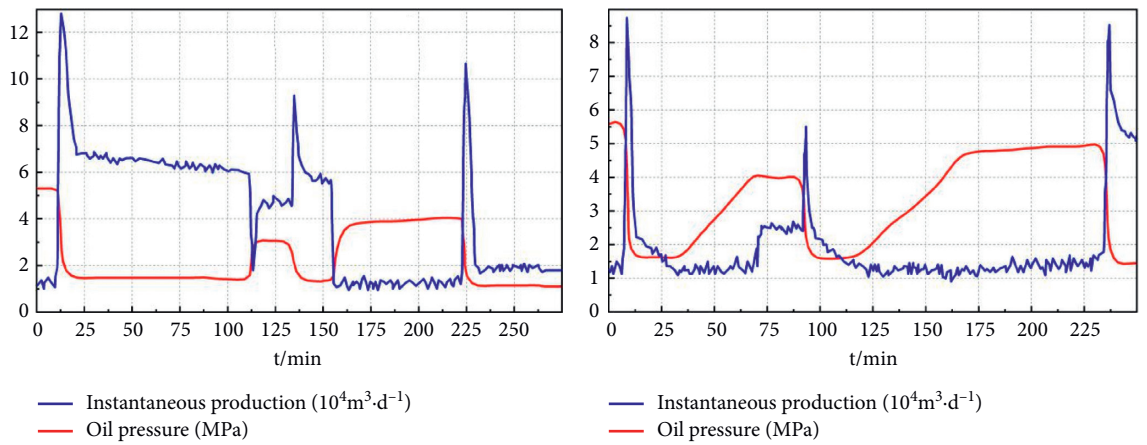

(a) (b)

Figure 14: Production regulation pressure waveform and production for 6 successive times. (a) Production regulation process with reducing opening. (b) Production regulation process with increasing opening.

figure, the throttle valve's flap is turned from 0° to 80°, indicating that the signal receiver at the head end successfully receives the pressure wave signal on the well. And then, it instructs the flap of the throttle vale to move, enabling wireless control of the opening change.

Based on Figure 14, the instantaneous production and the pressure wave signal have a correct correspondence relationship. It proves that the signal receipt accuracy is up to standard, and the noise immunity of the signal receiver meets the mining working condition requirement. The instantaneous production is up to the preset value, indicating that the flow capacity of the throttle is good, and no secondary throttling is formed at the annular flow passage between the air guide cylinder and the electric sealing cylinder, and the air moves up smoothly.

6. Conclusions

In order to ensure the fluid flow capacity of the wireless control downhole throttle and the noise immunity of the signal receiver, the author of this paper conducts numerical simulation of the flow field for the wireless control downhole throttle, focusing on the analysis of flow resistance characteristics of the annular flow passage between the air guide cylinder and the electric sealing cylinder as well as the stability of the flow field at the head end. The main conclusions drawn are as follows:

(i) Adjust the annular flow area by changing the outer diameter of the electric sealing cylinder to determine the critical effective cylinder diameter. Studies have shown that the outer diameter of the electric sealing cylinder cannot be higher than 36 mm. The critical effective working conditions of the throttle valve under the condition that the outer diameter of the electric sealing cylinder does not reach the critical effective cylinder diameter are analyzed. And the relations of the critical effective opening and changes of production before regulation are summarized, which may help guide the field operation.

(ii) Through the readings of the head monitor during the flow field simulation, the dynamic pressure fluctuation curves of different throttle openings and productions before regulation are plotted, and the dynamic pressure fluctuation range and mean value under different working conditions are summarized. The studies show that the maximum fluctuation of the dynamic pressure at the head end of the wireless control downhole throttle is less than 50 Pa, and the maximum dynamic pressure stability time is less than 5 s, with an average of ~3.3 s. According to the dynamic pressure trace diagram at the head end, the fluid flow here is relatively stable, and there is no obvious backflow and turbulence. It proves that signal reception is relatively reliable.

(iii) Field tests prove that the wireless control downhole throttle's production regulation capacity can be up to the presetting value. And again, the wireless control downhole throttle can accurately receive the pressure signal on the well, enabling downhole production regulation in a wireless and intelligent manner.

Data Availability

The simulation data used to support the findings of this study are available from the corresponding author upon request.

Conflicts of Interest

The authors declare that they have no conflicts of interest.

Acknowledgments

This study was supported by the Science and Technology Field Application Test Project of PetroChina Southwest Oil and Gas Field Company (20190303KS02).

References

[1] C. Dong, "Application of downhole throttle technology in fuling shale gas well," *China Petroleum and Chemical Standard and Quality*, vol. 39, no. 2, pp. 248–250, 2019.

[2] J. Ren, C. Li, and B. Li, "Application of downhole throttle technology for natural gas," *Petrochemical Industry Technology*, vol. 25, no. 6, p. 195, 2018.

[3] S. Li, *Natural Gas Engineering*, Petroleum Industry Press, Beijing, China, 2008.

[4] J. Qian, Z. Shen, W. Zhang et al., "Opportunity and challenge of intelligent completion technique in China," *Petroleum Geology and Engineering*, vol. 23, no. 2, pp. 76–79, 2009.

[5] C. Qu, Z. Wang, and J. Yuan, "The status and trends of intelligent completion well[J]," *Foreign Oil Filed Engineering*, vol. 26, no. 7, pp. 28–31, 2010.

[6] C. Bansal and A. Gandhe, "Intelligent web based task completion using pattern recognition techniques," *International Journal of Machine Learning and Computing*, vol. 2, no. 6, pp. 835–838, 2012.

[7] H. R. Saghir and S. B. Shouraki, "Self-organizing adaptive network-based fuzzy intelligent controller (soanfic)," *International Journal of Machine Learning and Computing*, vol. 2, no. 6, pp. 864–868, 2012.

[8] K. Gharehbaghi and K. Farnes, "Process automation in intelligent transportation system (ITS)," *International Journal of Machine Learning and Computing*, vol. 8, no. 3, pp. 294–297, 2018.

[9] A. Abdullatif and A. L. Omair, "*Economic evaluation of smart well technology*," M.S. thesis, Texas A&M University, College Station, TX, USA, 2007.

[10] C. Gao, Rajeswaran, and E. Nakagawa, "A literature review on smart-well technology," *SPE*, Article ID 106011, 2007.

[11] D.-X. Han, X.-F. Li, and L.-X. Fu, "Adaptability study of intelligent well systems in east China sea oil field," *International Journal of Plant Engineering and Management*, vol. 13, no. 4, pp. 205–213, 2008.

[12] M. He, F. Ma, and Y. Chen, "Design of intelligent downhole throttle control system," *Natural Gas and Oil*, vol. 31, no. 5, pp. 82–85+10, 2013.

[13] Z. Cai, X. Liao, and Y. Yuan, "Establishment of downhole throttle pressure drop model for gas wells," *Journal of Shaanxi*

University of Science & Technology (Natural Science Edition), vol. 31, no. 1, pp. 58–61, 2013.

[14] G. Li, Y. Zhang, Q. Li, and J. Li, "Model design of downhole adjustable sand control throttle," *Science Technology and Engineering*, vol. 11, no. 26, pp. 6453–6455, 2011.

[15] Y. Hu, Y. Huang, and X. Li, "Automatic de-noising and recognition algorithm for drilling fluid pulse signal," *Petroleum Exploration and Development Online*, vol. 46, no. 2, pp. 393–400, 2019.

[16] M. Zhu, S. Zhao, J. Li, and P. Dong, "Computational fluid dynamics and experimental analysis on flow rate and torques of a servo direct drive rotary control valve," *Proceedings of the Institution of Mechanical Engineers*, vol. 233, no. 1, pp. 213–226, 2018.

[17] W. Guo, "Study on linear regulating choke valve," *Drilling & Production Technology*, vol. 41, no. 3, pp. 75–78, 2018.

[18] C. Ye, D. Li, M. He, Y. Zhang, and X. Hu, "Production calculation method for gas wells with downhole throttle and its application," *Natural Gas Exploration & Development*, vol. 36, no. 3, pp. 58–60+3, 2013.

[19] C. Zhang, C. Zhang, S. Li, and F. Wang, "Study on calculation method of single well production in sulige gas field," *Natural Gas Technology and Economy*, vol. 5, no. 5, pp. 37–39+45+78, 2011.

[20] L. Xiao-Hui, "Test characteristics analysis of throttle opening test," *Hydraulics Pneumatics & Seals*, vol. 38, no. 3, pp. 13–15+12, 2018.

[21] S. Zhang, "Analysis on flow characteristics of throttle valve," *Valve*, no. 1, pp. 27-28, 2018.

[22] W. Liu, "Flow characteristic analysis of throttle valve," *Valve*, no. 2, pp. 20-21+23, 2017.

[23] Y. Wang, "Numerical simulation of the throttle valve flow field of natural gas wellheads," *Oil-Gas Field Surface Engineering*, vol. 37, no. 3, pp. 10–12, 2018.